EUMETSAT AC SAF
ATMOSPHERIC COMPOSITION MONITORING

PRODUCT USER MANUAL

GOME-2 surface LER product

Product Identifier	Product Name
O3M-402.1	Surface LER from GOME-2 / MetOp-A+B+C

Authors	Institute
L.G. Tilstra	Royal Netherlands Meteorological Institute (KNMI)
O.N.E. Tuinder	Royal Netherlands Meteorological Institute (KNMI)
P. Stammes	Royal Netherlands Meteorological Institute (KNMI)

Document status sheet

Issue	Date	Page(s)	Modified Items / Reason for Change
1.0	16-06-2014	all	first version of document
1.1	25-06-2014	all	changes and update after DRR
1.2	13-11-2014	6,7	added sections “Heritage” (1.2) and “Further information” (1.4)
1.3	24-10-2015	8–12	updated section 1.5 ; updated tables 1 and 2
2.0	24-11-2016	all	updated sections 3.1 and 3.2 ; added section 3.3
2.1	23-02-2017	all	updated sections 1.3, 1.6, 3.1, 3.2 and 4
2.2	02-05-2017	all	changes and update after DRR
3.0	26-09-2018	all	extended and updated sections 1–4 ; updated tables 1–5 ; added table 7 ; added figures 1 and 3 ; updated figure 2
3.1	26-03-2019	all	changes and update after DRR
3.2	08-05-2019	all	added description of NetCDF format ; added new section 3.5
4.0	01-12-2022	all	updated sections 1.2–1.4, 1.6, 1.7, 3.1–3.3, 3.5, 3.6 and 4 ; updated tables 1–3, 5
4.1	05-01-2023	8	version created for the review of O3M-402.1

Contents

Introduction to EUMETSAT Satellite Application Facility on Atmospheric Composition monitoring (AC SAF)

Background

The monitoring of atmospheric chemistry is essential due to several human caused changes in the atmosphere, like global warming, loss of stratospheric ozone, increasing UV radiation, and pollution. Furthermore, the monitoring is used to react to the threads caused by the natural hazards as well as follow the effects of the international protocols.

Therefore, monitoring the chemical composition and radiation of the atmosphere is a very important duty for EUMETSAT and the target is to provide information for policy makers, scientists and general public.

Objectives

The main objectives of the AC SAF is to process, archive, validate and disseminate atmospheric composition products (O_3, NO_2, SO_2, BrO, HCHO, H_2O, OClO, CO, NH_3), aerosol products and surface ultraviolet radiation products utilising the satellites of EUMETSAT. The majority of the AC SAF products are based on data from the GOME-2 and IASI instruments onboard MetOp satellites.

Another important task besides the near real-time (NRT) and offline data dissemination is the provision of long-term, high-quality atmospheric composition products resulting from reprocessing activities.

Product categories, timeliness and dissemination

NRT products are available in less than three hours after measurement. These products are disseminated via EUMETCast, WMO GTS or internet.

- Near real-time trace gas columns (total and tropospheric O_3 and NO_2, total SO_2, total HCHO, CO) and ozone profiles
- Near real-time absorbing aerosol indexes from main science channels and polarisation measurement detectors
- Near real-time UV indexes, clear-sky and cloud-corrected

Offline products are available within two weeks after measurement and disseminated via dedicated web services at EUMETSAT and AC SAF.

- Offline trace gas columns (total and tropospheric O_3 and NO_2, total SO_2, total BrO, total HCHO, total H_2O) and ozone profiles
- Offline absorbing aerosol indexes from main science channels and polarisation measurement detectors
- Offline surface UV, daily doses and daily maximum values with several weighting functions

Data records are available after reprocessing activities from the EUMETSAT Data Centre and/or the AC SAF archives.

- Data records generated in reprocessing
- Surface Lambertian-equivalent reflectivity
- Total OClO

Users can access the AC SAF offline products and data records (free of charge) by registering at the AC SAF web site.

More information about the AC SAF project, products and services: http://acsaf.org/

AC SAF Helpdesk: helpdesk@acsaf.org

Twitter: https://twitter.com/Atmospheric_SAF

1 Introduction

1.1 Document purpose and scope

This document is the Product User Manual (PUM) for the GOME-2 surface LER products developed at KNMI in the framework of the AC SAF (Satellite Application Facility on Atmospheric Composition Monitoring). The aim of this PUM is to present the data format used for the data record, and to explain and describe the contents of the fields contained in the database files.

1.2 Heritage

The GOME-2 surface LER product is the Lambertian-equivalent reflectivity (LER) of the Earth's surface observed by the GOME-2 instruments. It is the improved follow-up of earlier surface LER databases based on observations performed by GOME-1 (on the ERS-2 satellite) [*Koelemeijer et al.*, 2003] and OMI (on the Aura satellite) [*Kleipool et al.*, 2008].

The GOME-2 surface LER products are developed at KNMI in the framework of the AC SAF (Satellite Application Facility on Atmospheric Composition Monitoring). The algorithm described in the ATBD [*Tilstra et al.*, 2022a] is the direct continuation of the algorithms that were developed by *Koelemeijer et al.* [2003] and *Kleipool et al.* [2008]. Also see *Tilstra et al.* [2017, 2021].

1.3 GOME-2 surface LER product

Only one GOME-2 surface LER product is produced. Previously, separate products were produced for each GOME-2 instrument. The current product is based on the combination of level-1 data from the GOME-2 instruments on the MetOp-A, MetOp-B, and MetOp-C satellites:

Product ID	Satellite	Platforms	Surface LER versions
O3M-402.1	GOME-2	MetOp-A + MetOp-B + MetOp-C	MSC & PMD

The GOME-2ABC surface LER product consists of two surface LER versions: one version based on GOME-2 observations by the Main Science Channels (MSCs) and one version based on GOME-2 observations by the Polarisation Measurement Devices (PMDs). The PMD-based version has the advantage over the MSC-based version that the surface LER is based on eight times as many observations, each with an eight times smaller footprint. This makes the retrieved surface LER less susceptible to residual cloud contamination, statistically more stable, and therefore more reliable. It also allows a higher spatial resolution of the intrinsic surface LER database grid.

On the other hand, the surface LER of the PMD-based version is available only for a fixed list of wavelength bands. The wavelengths of the PMD bands are given in Table 4. This limitation is not an issue for the MSC-based surface LER. Here the list of wavelength bands could be determined based on user needs, taking into account that the wavelength bands have to be positioned in the continuum, avoiding strong absorption bands. The selected wavelength bands are given in Table 3.

1.4 Database versions

Table 1 provides an overview of the database versions that have been produced. The second column indicates which of these versions were officially released by the AC SAF after a review.

Version number	AC SAF release	MetOp satellites used / supported	Description ; Comments
1.0		A	first version ; created for testing purposes only
1.1	Yes	A	version released by the O3M SAF after review ; Product ID: O3M-89 ; various improvements were implemented after the initial testing phase
1.2		A	improved handling of residual clouds ; improved handling of missing data in polar night ; added a few wavelength bands after user requests
1.3		A	improved detection of cloud contamination ; much better handling of missing data in polar night ; minor changes to the data format
1.4		A	ozone taken from L2 product instead of from assimilated fields ; better treatment of missing data via snow/ice constraint on potential donor cells
1.5		A	improved error calculation (uncertainty field)
1.6		A	further fine-tuned treatment of missing data
1.7		A	switched to 32-bit floats and applied h5repack
2.0		A & B	higher spatial resolution near coastlines ; minor changes to the data format
2.1	Yes	A & B	version released by the O3M SAF after review ; Product IDs: O3M-89.1 and O3M-90 (MetOp-A and MetOp-B, respectively)

2.2		A & B	added wavelength bands at 685, 697, and 712 nm after user requests to support O_2-B band retrievals ; switch to L2 ozone from GDP 4.8
2.3		A & B	improved look-up tables: absorption by O_2 and H_2O taken into account (697/712 nm) + spectral calculation (328/697/712 nm) ; access to monthly water vapour climatology ; minor other changes to the code
2.4		A & B	added wavelength band at 585 nm to support O_2-O_2 band retrievals ; improved error calculation: separation of systematic and statistical errors
2.5		A & B	introduced 2D interpolation scheme to help users calculate surface albedo for their satellite footprints
3.0		A + B	directionality of LER implemented ; first version to combine GOME-2A and GOME-2B data
3.1	Yes	A + B	version released by the AC SAF after review ; switch to NetCDF format ; Product ID: O3M-402
4.0		A + B + C	first version to combine GOME-2A, GOME-2B, and GOME-2C data (covering 2007–2022)

Table 1: Overview of the database versions that were produced. Only versions 1.1, 2.1, and 3.1 have been officially released by the AC SAF. A MetOp-B database was first introduced for data version 2.0. As of version 3.0, the database that is produced is based on data from all of the available GOME-2 instruments. That is, the database is representative for all GOME-2 instruments (A, B, C).

1.5 Further information

1.5.1 The AC SAF website

Further up-to-date information and documentation on the GOME-2 surface LER products are available on the AC SAF website via the following URL:

http://acsaf.org

Requests for data and questions with regards to AC SAF products should be directed to the user services. Contact information is also available on the website mentioned above.

Important note:

Before 1 March 2017, the AC SAF had a different name: Satellite Application Facility on Ozone and Atmospheric Chemistry Monitoring (O3M SAF). As of 1 March 2017, this name should no longer be used. Please remember to update your acknowledgement (see section 1.5.2).

1.5.2 Acknowledgement instructions

When AC SAF data are used for operational or scientific purposes, the source of these data should be acknowledged. For example: "The data of the GOME-2 Lambertian-equivalent reflectivity (LER) are provided by KNMI in the framework of the EUMETSAT Satellite Application Facility on Atmospheric Composition Monitoring (AC SAF)".

1.6 Suggested reading material

Herman, J. R., and E. A. Celarier (1997), Earth surface reflectivity climatology at 340–380 nm from TOMS data, *J. Geophys. Res., 102*(D23), 28,003–28,011, doi:10.1029/97JD02074.

Koelemeijer, R. B. A., J. F. de Haan, and P. Stammes (2003), A database of spectral surface reflectivity in the range 335–772 nm derived from 5.5 years of GOME observations, *J. Geophys. Res., 108*(D2), 4070, doi:10.1029/2002JD002429.

Gao, F., C. B. Schaaf, A. H. Strahler, A. Roesch, W. Lucht, and R. Dickinson (2005), MODIS bidirectional reflectance distribution function and albedo Climate Modeling Grid products and the variability of albedo for major global vegetation types, *J. Geophys. Res., 110*, D01104, doi:10.1029/2004JD005190.

Kleipool, Q. L., M. R. Dobber, J. F. de Haan, and P. F. Levelt (2008), Earth surface reflectance climatology from 3 years of OMI data, *J. Geophys. Res., 113*, D18308, doi:10.1029/2008JD010290.

Popp, C., P. Wang, D. Brunner, P. Stammes, Y. Zhou, and M. Grzegorski (2011), MERIS albedo climatology for FRESCO+ O2 A-band cloud retrieval, *Atmos. Meas. Tech., 4*, 463–483, doi:10.5194/amt-4-463-2011.

Tilstra, L. G., O. N. E. Tuinder, P. Wang, and P. Stammes (2017), Surface reflectivity climatologies from UV to NIR determined from Earth observations by GOME-2 and SCIAMACHY, *J. Geophys. Res. Atmos., 122*, 4084–4111, doi:10.1002/2016JD025940.

Tilstra, L. G., O. N. E. Tuinder, P. Wang, and P. Stammes (2017), Surface albedo databases determined from PMD measurements performed by the GOME-2 instrument, *Proceedings of the 2017 EUMETSAT Meteorological Satellite Conference,* EUMETSAT, Rome, Italy, 2017.

Tilstra, L. G., O. N. E. Tuinder, P. Wang, and P. Stammes (2021), Directionally dependent Lambertian-

equivalent reflectivity (DLER) of the Earth's surface measured by the GOME-2 satellite instruments, *Atmos. Meas. Tech., 14*, 4219–4238, doi:10.5194/amt-14-4219-2021.

1.7 Abbreviations and acronyms

AAH	Absorbing Aerosol Height
AAI	Absorbing Aerosol Index
AC SAF	Satellite Application Facility on Atmospheric Composition Monitoring
AOT	Aerosol Optical Thickness
ATBD	Algorithm Theoretical Basis Document
BBA	Biomass Burning Aerosol
BRDF	Bidirectional Reflectance Distribution Function
BSA	Black-Sky Albedo
CDOP	Continuous Development & Operations Phase
COT	Cloud Optical Thickness
DAK	Doubling-Adding KNMI
DDA	Desert Dust Aerosols
DOAS	Differential Optical Absorption Spectroscopy
DU	Dobson Units, 2.69×10^{16} molecules cm^{-2}
ENVISAT	Environmental Satellite
EOS-Aura	Earth Observing System – Aura satellite
ERS	European Remote Sensing Satellite
ESA	European Space Agency
ETOPO-4	Topographic & Bathymetric data set from the NGDC, 4 arc-min. resolution
EUMETSAT	European Organisation for the Exploitation of Meteorological Satellites
FOV	Field-of-View
FRESCO	Fast Retrieval Scheme for Clouds from the Oxygen A band
FWHM	Full Width at Half Maximum
GMTED2010	Global Multi-resolution Terrain Elevation Data 2010
GOME	Global Ozone Monitoring Experiment
HDF	Hierarchical Data Format
IT	Integration Time
KNMI	Koninklijk Nederlands Meteorologisch Instituut
LER	Lambertian-Equivalent Reflectivity
LUT	Look-Up Table
MERIS	Medium Resolution Imaging Spectrometer
METOP	Meteorological Operational Satellite

MLS	Mid-Latitude Summer
MSC	Main Science Channel
NETCDF	Network Common Data Form, NetCDF
NGDC	NOAA's National Geophysical Data Center (Boulder, Colorado, USA)
NISE	Near-real-time Ice and Snow Extent
NOAA	National Oceanic and Atmospheric Administration
NRT	Near-Real-Time
OMI	Ozone Monitoring Instrument
O3M SAF	Satellite Application Facility on Ozone and Atmospheric Chemistry Monitoring
PMD	Polarisation Measurement Device
PSD	Product Specification Document
PUM	Product User Manual
RAA	Relative Azimuth Angle
RMSE	Root-Mean-Square Error
RTM	Radiative Transfer Model
SAA	Solar Azimuth Angle
SCIAMACHY	Scanning Imaging Absorption Spectrometer for Atmospheric Chartography
SZA	Solar Zenith Angle
TBA	To be Added
TBC	To be Confirmed
TBD	To be Defined
TEMIS	Tropospheric Emission Monitoring Internet Service
TOA	Top-of-Atmosphere
TOMS	Total Ozone Mapping Spectrometer
UTC	Coordinated Universal Time
UV	Ultraviolet
VAA	Viewing Azimuth Angle
VIS	Visible
VR	Validation Report
VZA	Viewing Zenith Angle

2 Surface reflectivity databases for the UV-VIS

2.1 Introduction

Surface reflectivity databases are needed for cloud, aerosol and trace gas retrievals. One of the first surface reflectivity databases retrieved using UV satellite remote sensing techniques is the Total Ozone Mapping Spectrometer (TOMS) [*Heath et al.*, 1975] surface LER database [*Herman and Celarier*, 1997]. The retrieved reflectivity is the Lambertian-equivalent reflectivity (LER) of the surface found from scenes which are assumed to be cloud free. The retrieval method relies on the removal of the (modelled) atmospheric contribution from the (observed) top-of-atmosphere (TOA) reflectance. In this approach the surface is defined to behave as a Lambertian reflector. The TOMS surface LER database ($1.25^\circ \times 1^\circ$) was retrieved for 340 and 380 nm only, which limits its usefulness.

The GOME [*Burrows et al.*, 1999] surface reflectivity database provides the surface LER on a $1^\circ \times 1^\circ$ grid for 11 wavelength bands between 335 and 772 nm [*Koelemeijer et al.*, 2003]. Although this is already quite an improvement with respect to the TOMS surface LER database, the database is still limited in quality by the low number of measurements from which the surface LER had to be extracted and the large GOME footprint size (see Table 2). In particular, pixels over sea are often affected by residual cloud contamination. In these cases the surface LER was retrieved from scenes which were not sufficiently cloud free. In other cases, e.g. snow surfaces, the surface LER was retrieved from a few measurements which were not representative for the entire month.

A large improvement on these points is the OMI surface reflectivity database [*Kleipool et al.*, 2008]. First, the OMI instrument [*Levelt et al.*, 2006] has a much smaller footprint size (24×13 km^2 at nadir) combined with a larger global coverage (see Table 2). This leads to better statistics and results in a higher accuracy for the surface LER retrieval. Second, the higher number of measurements allows for inspecting the distribution of scene LERs for each grid cell, and for making a more sophisticated selection of representative (cloud-free) scenes instead of directly taking the minimum scene LER value like in the case of the TOMS and GOME databases. Third, the provided OMI surface LER database has a higher spatial resolution ($0.5^\circ \times 0.5^\circ$ grid). The limiting factor is the OMI wavelength range. The longest wavelength in the OMI surface LER database is 499 nm.

The GOME-2 series of satellite instruments does not have some of the limitations of the satellite instruments mentioned above and can be used to create a better, more reliable surface LER database [*Tilstra et al.*, 2017]. To be more specific, it has the spectral range of GOME but a much smaller footprint (80×40 km^2) which is constant over the full swath width. Additionally, the number of measurements that are available per longitude/latitude cell is smaller than that of OMI, but enough to perform a statistical analysis on the distribution of retrieved scene LERs. Developing the GOME-2 surface LER retrieval the approach used for the OMI surface LER database was followed.

The main advantage of the GOME-2 surface LER database with respect to the OMI surface LER database is the wider wavelength range of the GOME-2 instrument. Additionally, the retrieval algorithm uses aerosol information, available via the GOME-2 Absorbing Aerosol Index (AAI) product, to filter out scenes with large aerosol loadings, as these scenes can result in inaccurate values of the retrieved surface LER. This filtering is especially important for locations over desert areas.

2.2 Tables

In Table 2 we summarise the properties of the discussed surface reflectivity databases. For GOME-2 we provide the specifications for the MSC-based and PMD-based algorithms. In Table 3 we list the wavelength bands of the surface reflectivity databases, and their application. In Table 4 we provide the wavelengths of the GOME-2 PMD bands, relevant to the PMD-based algorithm. The selection of the wavelength bands for the GOME-2 MSC-LER was influenced largely by the already existing surface LER databases. Below 325 nm the surface contribution to the TOA reflectance is low, which prevents an accurate retrieval of the surface LER below this wavelength. For the GOME-2 PMD-LER this means that the surface LER for PMDs 1–3 cannot be retrieved, as indicated.

instrument	TOMS	GOME	OMI	MSC - GOME-2 - PMD	
satellite	Nimbus-7	ERS-2	Aura	MetOp-A/B/C	
equator crossing time (LT)	12:00	10:30	13:45	09:30	
dayside flight direction	S→N	N→S	S→N	N→S	
number of days for global coverage	1	3	1	1.5	
pixel size at nadir (km × km)	50 × 50	320 × 40	24 × 13	80 × 40	10 × 40
number of usable pixels per orbit	∼12000	∼1300	∼83000	∼11000	∼88000
dataset time range (*)	1978–1993	1995–2000	2004–2007	2007–2022	2008–2022
selected wavelength bands	2	11	23	27	12
wavelength range covered (nm)	340–380	335–772	328–499	328–772	333–799
band width (nm)	1.0	1.0	1.0	1.0	see text
spatial resolution (°lon × °lat)	1.25 × 1.0	1.0 × 1.0	0.5 × 0.5	1.0 × 1.0	0.5 × 0.5
reference	HC1997	KHS2003	KDHL2008	TTWS2017/2021	

Table 2: Characteristics and properties of the UV-VIS surface LER databases, and of the satellite instruments from which they are derived. Wavelength band information can be found in Tables 3/4.

(*)The longer the time period covered, the higher the number of times a certain region has been observed. This increases the chances of having observed this region under clear sky conditions. Occasional reprocessing over longer time periods therefore increases the quality, stability, and reliability of the surface LER product. GOME-2A data are available from January 2007; GOME-2B data are available from November 2012; GOME-2C data are available from January 2019.

Table 3: Wavelength bands of the four monochromatic surface LER databases, and their applications. All wavelength bands are located outside strong gaseous absorption bands in order to avoid complicated modelling of the radiative transfer. The number of wavelength bands is also given.

λ (nm)	TOMS	GOME	OMI	GOME-2	application / relevance
328			+	+	LER, ozone, HCHO, SO_2
335		+	+	+	LER, ozone, HCHO
340	+			+	LER, aerosol, HCHO, BrO
342			+		LER, aerosol, HCHO, BrO
345			+		LER, aerosol, HCHO, BrO
354			+	+	LER, aerosol, HCHO, BrO, OClO
367			+	+	LER, aerosol, OClO
372			+		LER, aerosol, OClO
376			+		LER, aerosol, OClO
380	+	+	+	+	LER, aerosol, OClO
388			+	+	LER, aerosol, OClO
406			+		LER, aerosol
416		+	+	+	LER, aerosol
418			+		LER, aerosol
425			+	+	LER, aerosol, NO_2
440		+	+	+	LER, aerosol, NO_2
442			+		LER, aerosol, NO_2
452			+		LER, aerosol, NO_2
463		+	+	+	LER, aerosol, NO_2, O_2-O_2
471			+		LER, aerosol, NO_2, O_2-O_2
477			+		LER, aerosol, NO_2, O_2-O_2
488			+		LER, aerosol, NO_2, O_2-O_2
494		+	+	+	LER, aerosol, NO_2, O_2-O_2
499			+		LER, aerosol
510				+	LER, aerosol
526				+	LER, aerosol, vegetation
546				+	LER, aerosol, vegetation
555		+		+	LER, aerosol, vegetation
564				+	LER, aerosol, vegetation, O_2-O_2

585				+	LER, aerosol, vegetation, O_2-O_2, H_2O
610		+		+	LER, aerosol, H_2O
640				+	LER, aerosol, H_2O
670		+		+	LER, aerosol, H_2O, O_2-B
685				+	LER, aerosol, H_2O, O_2-B
697				+	LER, aerosol, H_2O, O_2-B
712				+	LER, aerosol, H_2O, O_2-B
747				+	LER, aerosol, O_2-A
758		+		+	LER, aerosol, O_2-A
772		+		+	LER, aerosol, O_2-A
Total:	2	11	23	27	

Table 3: Wavelength bands of the four monochromatic surface LER databases, and their applications. All wavelength bands are located outside strong gaseous absorption bands in order to avoid complicated modelling of the radiative transfer. The number of wavelength bands is also given.

The widths of the PMD bands are not provided in Table 4, but these (and other information) can be found in the "GOME-2 Factsheet" [*EUMETSAT*, 2021]. Additionally, Figure 1 provides a graphical representation of the spectral response functions of the PMD bands. The spectral response functions were determined using the slit functions of the individual detector pixels that make up the PMD bands. Note that we use the data from the PMD-p detector, not from the PMD-s detector. Ideally, PMD-p and PMD-s detectors should provide the same reflectance. In practice, they do not.

PMD	λ (nm)	application / relevance	PMD	λ (nm)	application / relevance
01	313	not retrieved	09	461	LER, aerosol, NO_2, O_2-O_2
02	318	not retrieved	10	520	LER, aerosol
03	325	not retrieved	11	555	LER, aerosol, vegetation
04	333	LER, ozone, HCHO	12	590	LER, aerosol
05	338	LER, aerosol, HCHO, BrO	13	640	LER, aerosol, H_2O
06	369	LER, aerosol, OClO	14	757	affected by O_2 absorption
07	382	LER, aerosol, OClO	15	799	LER, aerosol
08	414	LER, aerosol	PMD band definition v3.1, PMD-p detector		

Table 4: Wavelength information for the PMD bands used in the PMD-based surface LER algorithm. The wavelength definition follows PMD band definition v3.1, so the information applies to MetOp-A PMD data from after 11 March 2008 as well as to all MetOp-B and MetOp-C PMD data.

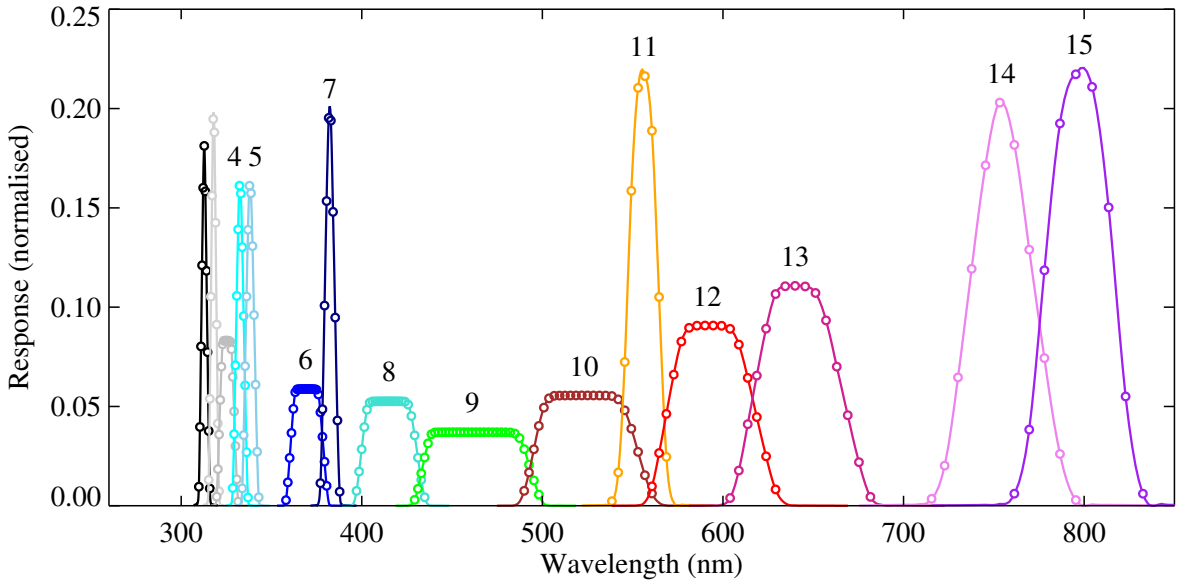

Figure 1: Spectral response functions of the fifteen GOME-2 PMD bands, determined using the slit functions of the underlying detector pixels of the PMD band. Only PMD bands 4–15 are labelled.

For some of the PMD bands the relatively broad wavelength range covered leads to inference with absorption bands. For instance, PMD 14 overlaps with the oxygen-A absorption band and this affects the retrieved surface LER. Likewise, PMD 15 is affected somewhat by water vapour absorption.

3 The GOME-2 surface LER product

3.1 Product files

For the GOME-2 surface LER data record (determined from the GOME-2 instruments on MetOp-A, MetOp-B, and MetOp-C, as explained in section 1.3) the MSC and PMD surface LER databases are separated into individual files. The GOME-2 surface LER product therefore consists of two files:

`GOME-2_MetOp-ABC_MSC_025x025_surface_LER_v4.0.nc` (2.3 Gb)
`GOME-2_MetOp-ABC_PMD_025x025_surface_LER_v4.0.nc` (1.6 Gb)

The file format of the GOME-2 surface LER product files is NetCDF-4. The fields that are contained in the product files are presented in Table 5 and are discussed in sections 3.2 and 3.3.

3.2 Contents of the product files

The *wavelength* field is an array listing the centre wavelengths of each of the wavelength or PMD bands. The width of the wavelength bands is typically 1.0 nm for the MSC-LER. For the PMD-LER, this width is by definition the width of the PMD band in question. More information about the PMD bands can be found in the "GOME-2 Factsheet" [*EUMETSAT*, 2021]. The number of wavelength bands (nwav) is either 27 (MSC-LER) or 12 (PMD-LER). The *longitude* and *latitude* arrays contain the centre longitudes or latitudes of the various grids contained in the product. The dimensions of the grids are defined by nlon=1440, nlat=720 for both the MSC-LER and the PMD-LER.

The *minimum_LER* and *mode_LER* fields hold the surface LER grids retrieved using the MIN-LER and MODE-LER approaches. As explained in the ATBD, the MIN-LER approach determines the surface LER in the traditional way in which the minimum scene LER that is found over time for a certain location is assumed to be representative for the surface LER. The MODE-LER approach analyses the distribution of retrieved scene LERs and, depending on the characteristics of the distribution and on the surface type, takes the mode or the minimum of the distribution. Over sea surfaces it always takes the minimum. Therefore, in most cases, the MODE-LER algorithm is identical to the MIN-LER algorithm. Nevertheless, there are differences over desert areas and snow/ice surfaces. The two approaches are explained more extensively in the ATBD. It is up to the user to decide which of the two surface LER grids suits best. Both are separately validated in the Validation Report.

Estimated uncertainties for the surface LER are provided in the two uncertainty fields. The *uncertainty_due_to_systematic_errors* is the estimated uncertainty in the surface LER due to systematic errors. It is calculated according to the method explained in section 8 of the ATBD. The *uncertainty _due_to_systematic_errors* is the estimated uncertainty in the surface LER due to statistical errors.

data set name	data type	description
month	string(nmon)	month (JANUARY . . . DECEMBER)
wavelength	float(nwav)	central wavelength of band
longitude	float(nlon)	centre longitude of row
latitude	float(nlat)	centre latitude of column
minimum_LER	float(nmon,nwav,nlon,nlat)	MIN-LER surface LER
mode_LER	float(nmon,nwav,nlon,nlat)	MODE-LER surface LER
uncertainty_due_to_systematic_errors	float(nmon,nwav,nlon,nlat)	estimated uncertainty due to systematic errors
uncertainty_due_to_statistical_errors	float(nmon,nwav,nlon,nlat)	estimated uncertainty due to statistical errors
flag	byte(nmon,nlon,nlat)	quality flag (0,1,2,3,4,5)
snow_ice_field	short(nmon,nlon,nlat)	surface flag (0,1,2,3,127,255)
polynomial_coefficients_index	byte(3)	index of coefficient (0,1,2)
polynomial_coefficients_minimum_LER	float(nmon,nwav,nlon,nlat,3)	DLER polynomial coefficients for the MIN-LER
polynomial_coefficients_mode_LER	float(nmon,nwav,nlon,nlat,3)	DLER polynomial coefficients for the MODE-LER

Table 5: Fields contained in the GOME-2 surface LER products. MSC-LER: nwav=27, nlon=1440, nlat=720; PMD-LER: nwav=12, nlon=1440, nlat=720. The number of months (nmon) is 12.

This uncertainty is the standard deviation of the scene LER values that were averaged to obtain the surface LER. Note that both uncertainty fields are calculated for (and from) the *mode_LER* field. The uncertainty fields for the *minimum_LER* are not provided, as they are very similar, and we want to minimise the product file size. The four types of grids described above are comprised of nmon $\times$ nwav $\times$ nlon $\times$ nlat values, where the number nmon=12 refers to the twelve calendar months found inside the *month* field. For the MSC-LER we have have the dimensions set to nwav=27, nlon=1440, nlat=720. For the PMD-LER the dimensions are nwav=12, nlon=1440, nlat=720.

An integer quality flag is provided in the *flag* field. The dimension of the matrix is nmon $\times$ nlon $\times$ nlat. Possible values range from 0 to 5. Table 6 explains the meaning of these flags. This table was taken directly from the ATBD. The ATBD provides a more complete description of the quality flag.

The *snow_ice_field* is a flag that indicates the surface conditions. The dimension of the matrix is nmon $\times$ nlon $\times$ nlat. Possible values are listed in Table 7 which explains the meaning of this indicator. The values are actually the values shown in the flowchart presented in green in Figure 2 of the ATBD. The values 0 (“land”) and 255 (“water”) were given to the grid cell when all measurements collected in the grid cell were classified as “land” or “water”, respectively. The values 1 (“permanent ice”), 2 (“sea ice”), and 3 (“snow”) were given according to the rules shown in the flowchart in Figure 2 of the

Flag	Meaning of flag
0	data are ok; no corrections applied
1	residual cloud contamination above ocean detected – replaced by nearby cloud-free cell
2	residual cloud contamination above ocean detected – no suitable replacement could be found (the pixel remains cloud contaminated and/or receives the LER spectrum of a less than optimal donor cell)
3	missing data for polar regions which are observed only part of the year – filled in using nearest month with reliable surface LER data
4	missing data throughout the entire year
5	suspect surface LER value retrieved for at least one of the wavelengths

Table 6: Definition of the quality flags that are provided along with the surface LER products.

Flag	Meaning of flag
-1	fill value; most likely due to a low number of measurements
0	grid cell classified as “land” in all cases
1	grid cell classified as “permanent ice”
2	grid cell classified as “sea ice”
3	grid cell classified as “snow”
127	grid cell undetermined: either changed nature during the month or coastline involved
255	grid cell classified as “water” in all cases

Table 7: Definition of the “snow_ice_field” flag. See text for further explanation.

ATBD. Grid cells that were not given one of these values were given a value of 127, indicating that the grid cell changed nature during the month. This could, for instance, be a transition from “land” to “snow”, or from “water” to “sea ice”. A value of 127 is also given when the grid cell contains a coastline. More information can be found in the ATBD.

The fields *polynomial_coefficients_index*, *polynomial_coefficients_minimum_LER*, and *polynomial_coefficients_mode_LER* shown in Table 5 are explained in the next section.

3.3 Directionally dependent surface LER (DLER)

The GOME-2 surface LER product contains, next to the traditional non-direction surface LER, also directionally dependent surface LER information. This DLER information provides the users with albedo values that are a function of the viewing direction, thereby essentially representing the surface BRDF of the scene. This only holds when the DLER is used for satellite observations which

were performed from polar satellite orbits that have similar equator overpass times as the MetOp satellites (09:30 LT). This includes, of course, satellite data originating from MetOp-A/B/C, for example data from GOME-2 or AVHRR, but also data from Envisat (10:00 LT), for example data from SCIAMACHY or AATSR, from ERS-2 (10:30 LT), for example data from GOME-1 or ATSR-2, or data from other polar satellites in morning orbits sufficiently close to an equator crossing time of 09:30 LT. The DLER approach cannot be used for satellites instruments in noon or afternoon orbits such as OMI or TROPOMI. Here users can only make use of the non-directional surface LER.

In the GOME-2 surface LER product the DLER surface albedo A_{DLER} is presented as a correction on top of the traditional non-directional surface LER field A_{LER}. The non-directional field A_{LER} can be either the *minimum_LER* or *mode_LER* field as discussed in section 3.2. The surface DLER is parameterised as a function of the (signed) viewing angle θ_{v} in the following way:

$$A_{\mathrm{DLER}} = A_{\mathrm{LER}} + c_0 + c_1 \cdot \theta_{\mathrm{v}} + c_2 \cdot \theta_{\mathrm{v}}^2 \,. \tag{1}$$

In this equation, θ_{v} is in an absolute sense equal to the viewing zenith angle θ, but expected to be negative on the east side of the orbit swath, and positive on the west side of the orbit swath. The user has to take care of this. For users that use GOME-2 MSC level-2 data, this means that for the nominal scans with 32 observations, the VZA of observations with an IndexInScan of 1–12 and 29–32 has to be multiplied by −1. For users that use the GOME-2 PMD bands, this has to be done for the observations with IndexInScan of 1–96 and 225–256. The VZA is to be provided in degrees.

The coefficients c_0, c_1, and c_2 are stored in the *polynomial_coefficients_minimum_LER* or the *polynomial_coefficients_mode_LER* field, depending on whether the user is interested in the MIN-LER or MODE-LER field. The dimension of the matrices is nmon × nwav × nlon × nlat × 3. For water bodies the coefficients c_0, c_1, and c_2 were set to zero. They were also set to zero for coastal areas and for areas for which the DLER could not be retrieved. More information can be found in the ATBD.

3.4 Intrinsic spatial resolution

The resolution of the grids provided in the surface LER products is $0.25^\circ \times 0.25^\circ$, for both the MSC-LER and the PMD-LER. The *intrinsic* resolution, however, is different. For the MSC-LER, the intrinsic resolution is $1^\circ \times 1^\circ$ for most non-coastal areas. For the coastal areas, the intrinsic resolution switches to $0.5^\circ \times 0.5^\circ$ near the coastline, and to $0.25^\circ \times 0.25^\circ$ at the coastline. See Figure 2. This dynamic gridding is performed in order to achieve a higher spatial resolution at the coastline.

As a result, the intrinsic spatial resolution of the MSC-LER is $1^\circ \times 1^\circ$, except for the coastline and for a few mountain ranges, where the intrinsic resolution is $0.25^\circ \times 0.25^\circ$. For the PMD-LER, the intrinsic spatial resolution for most non-coastal areas is $0.5^\circ \times 0.5^\circ$, and $0.25^\circ \times 0.25^\circ$ at the coastline, for some mountain areas, and for the Sahara desert. The intrinsic resolution of the PMD-LER is therefore

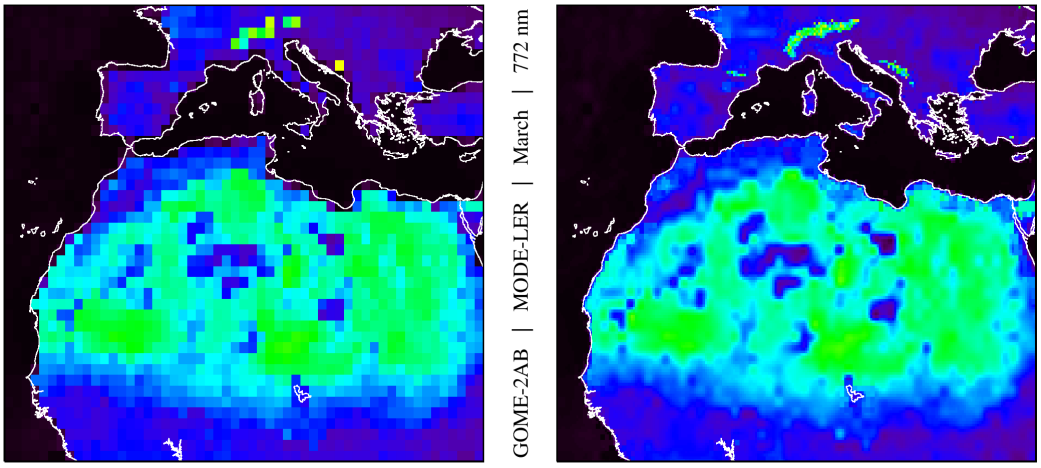

Figure 2: Surface LER retrieved at 772 nm, for the month March and presented for western Europe. Left: original one-degree resolution; Right: increased resolution of 0.25-degrees.

higher than that of the MSC-LER, even though the size of their grids is identical. The method that is used to control the intrinsic spatial resolution via dynamic gridding is explained in the ATBD.

After the dynamic gridding is performed, the grids are smoothed by a bilinear interpolation method. *Because of this, users do not need to worry about the differences in intrinsic resolution of the surface LER grids when they want to link the database grid cells to the measurements footprints of their observations*. The interpolation scheme was first introduced in version 2.5 of the database.

3.5 Previous releases and alternative data format (HDF-5)

For early previous releases of the GOME-2 surface LER databases (see Table 1) the file format that was used was HDF-5. The current release is still available in this format for users that are used to the HDF-5 format, but only upon request. For the current release the available HDF-5 files are:

`GOME-2_MetOp-ABC_MSC_025x025_surface_LER_v4.0.hdf5`	(2.6 Gb)
`GOME-2_MetOp-ABC_PMD_025x025_surface_LER_v4.0.hdf5`	(1.6 Gb)

Older, previous databases that were officially released by the AC SAF are:

`GOME-2_MetOp-A_MSC_025x025_surface_LER_v2.1.hdf5`	(617 Mb)
`GOME-2_MetOp-A_PMD_025x025_surface_LER_v2.1.hdf5`	(656 Mb)
`GOME-2_MetOp-B_MSC_025x025_surface_LER_v2.1.hdf5`	(609 Mb)
`GOME-2_MetOp-B_PMD_025x025_surface_LER_v2.1.hdf5`	(652 Mb)
`GOME-2_MetOp-AB_MSC_025x025_surface_LER_v3.1.hdf5`	(2.5 Gb)
`GOME-2_MetOp-AB_PMD_025x025_surface_LER_v3.1.hdf5`	(1.6 Gb)

These older releases differ from the current version in various ways, as described in section 1.4. The most important difference for v2.1, however, is that these older databases only contain the surface LER, and not the surface DLER. Apart from this, the quality of the older databases is also lower than that of the current version. We therefore recommend to always use the most recent version available.

The fields that are contained in the database files are presented in Table 5 and are discussed extensively in sections 3.2 and 3.3. Note, however, that the order of the dimensions in the fields inside the HDF-5 files is reversed w.r.t. the order used in the NetCDF files.

3.6 User guideline

Since version 3.0 of the GOME-2 surface LER database only one database exists, which is based on data from all GOME-2 instruments (A, B, C). The MSC-LER will be the most logical choice for most users. The PMD-LER is intended for users that need surface albedo input for their (GOME-2) PMD band retrievals, or that really need the higher intrinsic resolution of the PMD-LER.

The choice between MIN-LER or MODE-LER is more difficult and depends on the application at

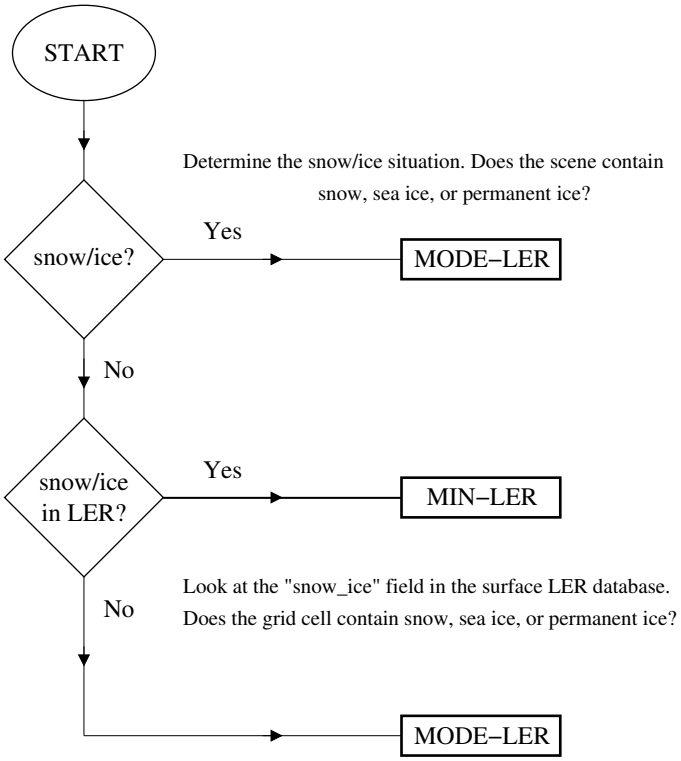

Figure 3: Flowchart describing how to decide between MIN-LER and MODE-LER fields.

hand. For most users the MODE-LER is the better choice over desert areas. For snow/ice situations it is not always clear which of the two albedo fields is better. The MIN-LER always represents the situation of minimum snow/ice presence. The MODE-LER on the other hand represents the situation of snow/ice cover already when only a fraction of the time snow/ice was present. The MIN-LER and MODE-LER databases therefore span up a range of possible snow/ice cover.

Figure 3 presents a flowchart which can be used by users of the GOME-2 surface LER database to handle the different situations that may occur. If the scene at hand contains snow or ice, then the MODE-LER needs to be used, as the MODE-LER is more representative for the average snow/ice situation than the MIN-LER. If the scene does not contain snow, then we look at the *snow_ice_field*. If this field indicates snow or ice at the relevant location, then the MIN-LER is most suited, as the MIN-LER represents the situation of minimal snow presence. If snow is not present in the scene and also non according to the *snow_ice_field*, then the MODE-LER is used because for desert scenes it is better to use the MODE-LER (and for other snow-free scenes the two fields are identical).

More details and background information can be found in *Tilstra et al.* [2017, 2021].

4 Product quality

The validation approach and the methods that were used to get to the results are described extensively in *Tilstra et al.* [2017, 2021]. A report on the most current product quality can be found in the Validation Report (VR) [*Tilstra et al.*, 2022b]. For the GOME-2 surface LER database, the results presented in this VR indicate that the GOME-2ABC MSC MIN-LER and MODE-LER surface LER products are in general accurate within 0.01 over the ocean and accurate within 0.04 over snow/ice surfaces. These numbers were derived on the basis of comparisons of the GOME-2ABC surface LER database with the established GOME-1 and OMI surface LER databases.

For the PMD-LER database, the comparison with OMI and with the GOME-2ABC MSC-LER showed a good agreement for all PMD bands. The results indicate that the PMD-LER has improved slightly compared to the previous version 3.1. This holds for all PMD bands and is a direct result of the larger amount of data included in the creation of the database.

For the individual locations (grid cells) in the database, uncertainty fields are present in the database file containing the GOME-2 surface LER database. These uncertainty fields provide for each month of the year, for each wavelength band, and for each grid cell in the latitude/longitude grid, an estimation of the systematic and statistical uncertainties in the retrieved surface LER.

References

Burrows, J. P., et al. (1999), The Global Ozone Monitoring Experiment (GOME): Mission concept and first scientific results, *J. Atmos. Sci., 56*(2), 151–175.

EUMETSAT (2021), GOME-2 Factsheet, Doc. No. EUM/OPS/DOC/10/1299, Issue 4f, 14 December 2021, EUMETSAT, Darmstadt, Germany, https://www.eumetsat.int/media/47563.

Heath, D. F., A. J. Krueger, H. A. Roeder, and B. D. Henderson (1975), The Solar Backscatter Ultraviolet and Total Ozone Mapping Spectrometer (SBUV/TOMS) for NIMBUS G, *Opt. Eng., 14*(4), 144323, doi:10.1117/12.7971839.

Herman, J. R., and E. A. Celarier (1997), Earth surface reflectivity climatology at 340–380 nm from TOMS data, *J. Geophys. Res., 102*(D23), 28,003–28,011, doi:10.1029/97JD02074.

Kleipool, Q. L., M. R. Dobber, J. F. de Haan, and P. F. Levelt (2008), Earth surface reflectance climatology from 3 years of OMI data, *J. Geophys. Res., 113*, D18308, doi:10.1029/2008JD010290.

Koelemeijer, R. B. A., J. F. de Haan, and P. Stammes (2003), A database of spectral surface reflectivity in the range 335–772 nm derived from 5.5 years of GOME observations, *J. Geophys. Res., 108*(D2), 4070, doi:10.1029/2002JD002429.

Levelt, P. F., G. H. J. van den Oord, M. R. Dobber, A. Mälkki, H. Visser, J. de Vries, P. Stammes, J.O.V. Lundell, and H. Saari (2006), The Ozone Monitoring Instrument, *IEEE Trans. Geosci. Remote Sens., 44*(5), 1093–1101, doi:10.1109/TGRS.2006.872333.

Popp, C., P. Wang, D. Brunner, P. Stammes, Y. Zhou, and M. Grzegorski (2011), MERIS albedo climatology for FRESCO+ O2 A-band cloud retrieval, *Atmos. Meas. Tech., 4*, 463–483, doi:10.5194/amt-4-463-2011.

Tilstra, L. G., O. N. E. Tuinder, P. Wang, and P. Stammes (2017), Surface reflectivity climatologies from UV to NIR determined from Earth observations by GOME-2 and SCIAMACHY, *J. Geophys. Res. Atmos., 122*, 4084–4111, doi:10.1002/2016JD025940.

Tilstra, L. G., O. N. E. Tuinder, P. Wang, and P. Stammes (2021), Directionally dependent Lambertian-equivalent reflectivity (DLER) of the Earth's surface measured by the GOME-2 satellite instruments, *Atmos. Meas. Tech., 14*, 4219–4238, doi:10.5194/amt-14-4219-2021.

Tilstra, L. G., O. N. E. Tuinder, and P. Stammes (2022a), GOME-2 surface LER product – Algorithm Theoretical Basis Document, *KNMI Report SAF/AC/KNMI/ATBD/003*, Issue 4.0, November 30, 2022.

Tilstra, L. G., O. N. E. Tuinder, and P. Stammes (2022b), GOME-2 surface LER product – Validation Report, *KNMI Report SAF/AC/KNMI/VR/002*, Issue 1/2022, December 2, 2022.